Volcanic strain change prior to an earthquake swarm observed by groundwater level sensors in Meakan-dake, Hokkaido, Japan

Hiroaki Takahashi[a], Tomo Shibata[b], Teruhiro Yamaguchi[a], Ryuji Ikeda[a], Noritoshi Okazaki[b], and Fujio Akita[b]

[a] *Institute of Seismology and Volcanology, Hokkaido University, Sapporo, Japan*

[b] *Geological Survey of Hokkaido, Sapporo, Japan*

Abstract

We installed and operated a low-cost groundwater level observation system at intermittent hot spring wells in order to monitor volcanic strain signals from the active Meakan-dake volcano in eastern Hokkaido, Japan. Data are sampled at 1 Hz and are transmitted to the data center in real time. Evaluation of the water level time series with theoretical predictive tidal strain and coseismic static strain changes has suggested that the wells penetrate to the artesian aquifer and act as a volumetric strain sensor. An active earthquake swarm with more than 400 events occurred at the shallower part of the volcano from January 9 to 11, 2008. Three independent wells recorded pre- to co-swarm groundwater drops simultaneously, which represented a decrease in volumetric strain. The total volumetric strain change during the three active days was estimated to be from 6 to 7×10^{-7}. The observed data, including changes in volumetric strain, absence of deformation in the GPS coordinates, and activation of deep low-frequency earthquakes, might imply possible deflation of a source deeper than 10 km, and these preceding deeper activities might induce an earthquake swarm in a shallower part of the

Meakan-dake volcano.

1. Introduction

The Meakan-dake volcano in eastern Hokkaido, Japan, is an active volcano with an elevation of 1,499 m (Fig. 1). The Meakan-dake volcano is a typical island-arc volcano associated with the subducting Pacific plate. Although historical records are limited, several phreatic eruptions have been recorded since 1955. Effusive rock compositions of this volcano are dacite, andesite, and basaltic andesite (Wada, 1991). Three major stages of explosive eruptive activity at 12 ka, 9 ka, and 5 to 6 ka were associated with the generation of pyroclastic flows, and successive lava effusions have continued fitfully over the last few thousand years. The most recent magmatic eruption was estimated to have occurred anywhere from several hundreds of years to thousands of years ago (Wada et al., 1997).

In 1956, the Japan Meteorological Agency (JMA) installed a seismograph, which has been operated routinely since 1973. The number of earthquakes per day sometimes exceeded 400 when an active earthquake swarm occurred (Fig. 2a). However, none of these earthquakes were felt because of their miniscule magnitude. Small phreatic eruptions in 1988, 1996, 2006 and 2008 occurred following an earthquake swarm.

Geothermal fields and hot springs are located on and near the volcanic edifice. Prior to 2004, the average temperature of active fumaroles in the summit crater (Fig. 1) had been approximately 400°C (Fig. 2b). However, a decrease in temperature was observed over the last decade, and recent data gathered during the spring of 2008 indicated that the temperature was less than 100°C (Fig. 2b).

Crustal deformation associated with volcanic activity can be used to investigate the

magmatic and/or geothermal system beneath the volcanic edifice. However, recent space geodetic techniques such as GPS and InSAR provide high-quality geodetic data, strain observations can provide higher precise signals that cannot be detected by GPS (e.g., Agnew and Wyatt, 2003, Ueda et al., 2005, Chardot et al., 2010). Although high installation cost is one of main difficulties in establishing a new site, Hokkaido University and the Geological Survey of Hokkaido started a low-cost groundwater level change observation at intermittent hot spring wells to monitor the strain activity of the Meakan-dake volcano. We herein report a volcanic strain event determined using the newly proposed groundwater observation system.

2. Groundwater level observation

Several studies have shown that, under proper conditions, artesian groundwater acts as a volumetric strain sensor (Wakita, 1975, Roeloffs, 1988, Quilty and Roeloffs, 1997, Matsumoto et al., 2002, 2003, Akita and Matsumoto, 2004, Itaba et al., 2010, Shibata et al., 2010, Gahalaut et al., 2010). The suggested volcanic strain signals might also be observed as groundwater level changes. In order to monitor volcanic unrest signals using groundwater level data, we used three preexisting intermittent hot spring water wells, AK1, AK3, and AK4, which are situated approximately 8 km NNE from the volcano summit (Fig. 1). The parameters of each well are listed in Table 1 (Kawamori et al., 1987). Well AK1 had a borehole depth of 1,061 m with a strainer located at a depth of between 518 and 1,061 m, whereas wells AK3 and AK4 had shallower boreholes (92 and 57 m) with strainers located at depths of between 24 and 55 m and between 41 and 57 m, respectively. These facts indicate that AK1 and AK3-4 penetrate different aquifers. In order to measure the groundwater levels, in April of 2006, we installed a water

pressure measurement sensor (Druck PTX1830) approximately 5 m below the water surface. The hydraulic heads from the ground surface are 1 m for AK1 and 0.5 m for AK3 and AK4. The sensor resolution is less than 1 mm. A barometric pressure sensor was also deployed at the same location in order to eliminate barometric pressure effects on the water levels. The obtained data are converted to digital signals using a 24-bit AD converter at a sampling rate of 1 Hz and are transmitted in real time to the data center at Hokkaido University via IP protocol. A precise time calibration is accomplished by on-site GPS receivers every two hours. All data are stored in a crustal deformation database system (Yamaguchi et al., 2010) and are distributed to concerned institutions in pseudo-real time.

The proportion of the groundwater level to crustal strain was evaluated by Saito (2008). He analyzed raw water level data for a period of one month using BAYTAP-G tidal analysis software (Ishiguro et al., 1981, Tamura et al., 1991). The time series of the tidal response, the barometric pressure response, and the irregular and trend components were deconvoluted. The barometric component was obtained using barometric pressure data observed at the observation site. Clear responses to tidal components were observed at AK1 and AK4, suggesting that these wells are under artesian influence. In contrast, a less clear response was observed at AK3, indicating that this well is not under artesian influence. Based on these observations, Saito (2008) concluded that the sensitivity coefficients of the M2 tidal component (period: 12.42 hours) were dominant and had a smaller phase difference. The coefficients of volumetric strain to the groundwater level were estimated by comparing the theoretical volumetric tidal strains of earth and ocean loading calculated using GOTIC2 tidal loading computation software (Matsumoto et al., 2001), and the observed tidal components were decomposed by

BAYTAP-G software. The strain sensitivities to the M2 tidal constituent, W_s, were calculated as follows:

$W_s = T_w/T_t$,

where T_w and T_t are the water level and theoretical amplitude of the M2 tidal component, respectively (Table 1).

In order to validate the above procedure, a suitability test of the response coefficient was conducted by comparing coseismic water level changes with theoretical values observed at AK1. The result also indicated properness of the water level coefficients to volumetric strain. In addition, a suitability test by Saito (2008) revealed that the actual coseismic response of AK4 was not consistent with the theoretical values, and he suggested applying an inflow model to this well. The above considerations indicate that AK1 has a good response to strain changes for a wide range of periods, whereas AK4 has a good response only for phenomena having a period longer than the M2 tide. The observations on AK3 can be used as supplemental data.

3. Volcanic earthquake swarm and groundwater level changes

An earthquake swarm began at 17:00 on January 9, 2008. Note that we hereinafter use Japan Standard Time (JST) (GMT+9). The number of earthquakes increased until 12:00 January 10 and then decreased until 23:00 January 10. The hypocenters of the volcanic earthquakes determined by the Sapporo district Meteorological Observatory (SMO) of the JMA volcano observation network were concentrated just under the summit crater at an elevation of 0 to 0.5 km (Fig. 3). The maximum number of hourly earthquakes exceeded 40, and the total number of earthquakes over a three-day period was 624. None of the earthquakes were felt because the maximum magnitude was less than 0.5.

Webcams installed by the JMA and other institutes did not capture any anomalous activity, such as smoke escaping from active vents. Moreover, the GPS stations operated by the JMA did not detect any signals during this swarm (Fig. 4).

Prior to this earthquake swarm, the lowering of the groundwater level began at the three wells simultaneously, indicating a decrease in volumetric strain. Figure 5 shows the changes in the original water levels, the barometric pressure, and the corrected water levels of AK1 for two weeks before and after the event. Although a clear water level decrease was observed in the original record corresponding to the swarm activity around January 10, the fluctuation of the water level was influenced by barometric pressure and tidal strain. In order to eliminate these noises in the groundwater level data, we applied BAYTAP-G tidal analysis software with barometric pressure data (Ishiguro et al., 1981, Tamura et al., 1991). Note that no precipitation effect was considered because snow cover was observed until mid-December. Figure 6 indicates the corrected water levels of the three wells. These independent wells showed the water decreasing coherently. This should correspond to a real phenomenon because the three wells are spatially independent and have different depths. Figure 6 also shows the dilatational strain recorded by a quartz tube strain meter at a nearby TES station located 25 km east of the AK wells (Fig. 1b). Comparison with TES dilatation clearly indicated that the groundwater signals at the AK wells were not tied to regional phenomena (Fig. 6). Note that the linear dilatational trend at the TES station is a portion of secular deformation signal. The above consideration strongly suggests that these water signals were related to local events induced by the volcanic unrest of the Meakan-dake volcano.

Changes at the three wells appeared to begin before earthquake swarm occurrence. A differential rate of water level change at AK1 indicated that the water table fall started at

20:00 January 8 (Fig. 6), which is approximately 21 hours prior to earthquake swarm initiation (Fig. 6). This clearly indicates that tensional dilatation had progressed at the AK wells without showing earthquake activity. The earthquake swarm began at almost the maximum water table drop during the period of interest. All of the water levels decreased and did not recover until at least 20 January. The amplitudes of the total water decrease at AK1, AK3, and AK4 were approximately 25 cm, 3 cm, and 4 cm, respectively. The sensitivity coefficient difference (AK1 is 5.8 times larger than AK4) is consistent with that of the water level change values. In fact, the volumetric strain values calculated using the estimated sensitivity coefficients was of approximately the same order (Table 1).

The above results provide an idea of how to evaluate the unknown sensitivity of AK3. The AK wells are located in close proximity to each other relative to the distance to the deformation source location. This allows us to assume that the geometrical effect generated by source parameters is small. Hence, the volumetric strain changes at the three wells should be equivalent if the source exhibits radial symmetry. The coefficient of AK3 was estimated through comparison with the AK1 and AK4 water drop values (Table 1). This also implied that AK3 might act as a volumetric strain sensor for a period of a few days.

4. Discussion

The observed data strongly suggested that water level changes were related to the volcanic unrest of the Meakan-dake volcano. However, the biased location of the wells did not allow us to estimate the deformation source parameters of the strain event. The JMA have operated a continuous GPS network in this volcano for some time (Fig. 1).

169 Baseline length changes for a month including an earthquake swarm period suggested
170 that this network can detect a displacement signal of more than a few centimeters (Fig.
171 4). We assumed detection resolutions of 1 cm and 2 cm for the baseline and vertical
172 components, respectively. No significant displacement signals exceeding the above
173 resolutions were observed before, during, or after the swarm, which provides a strong
174 constraint for deformation source modeling.

175 We used water level and GPS data to estimate the depth and volume change of the
176 deformation source. A buried point source, the Mogi model (Mogi, 1958), was assumed
177 for modeling. The lack of GPS displacement for all of the baselines suggested that point
178 source location estimation based on these data would be impossible. The epicenters of
179 both the shallower earthquake swarm (Fig. 3) and the deep low-frequency earthquakes
180 (DLEs) were concentrated just beneath the summit crater. Wherefore, we fixed the
181 horizontal location of a point source to the summit crater a priori. The depth and volume
182 change were valuable for modeling. The displacement and strain field was computed
183 using Okada's (1992) formula, and the Poisson ratio and Lame's constant were set to
184 0.25 and $\mu = \lambda$, respectively.

185 We evaluated the variation change of root mean square (rms) residuals by changing the
186 depth and volume parameters following a grid-search procedure. The grid intervals were
187 set at 1 km for depth and 0.001 km^3 for volume change. We first examined a point
188 source at a depth of 3 km because the hypocenter depth of the earthquake swarm was
189 concentrated near sea level (Fig. 2). The depression volume of 0.004 to 0.005 km^3 well
190 explained the water level data, but coincidently induced a displacement of more than a
191 few centimeters on GPS baselines and vertical components. This was not consistent
192 with the observed data, and, as such, indicated that the water drop might not be due to

193 shallowest source deflation.

194 The rms distributions for each depth and volume change parameter are shown in Fig. 7.
195 Note that the rms for GPS baselines and vertical components were computed based on
196 the root-mean for the sum of each squared residual, and each rms is normalized by the
197 apparent value. The rms distribution of both GPS baselines (Fig. 7a) and the GPS
198 vertical component (Fig. 7b) exhibit bilateral symmetry, and a deeper source provides a
199 lower rms, which indicates that a deeper source is preferable to a shallower source. The
200 gradient rate along the lateral axis is also smaller for a deeper source and larger for a
201 shallower source.

202 On the other hand, the rms of the AK1 volumetric strain indicates an asymmetric
203 distribution (Fig. 7c). The left- and right-hand segments are due to the deflation and
204 inflation of the point source, respectively. Small, broad rms segments appear in the
205 left-upper side. This rms distribution indicates that deflation is preferable to inflation.
206 The local rms minimum appearing in right-lower side might not be correct because of
207 the inconsistency with the rms maps of GPS baselines and vertical data. However, these
208 three rms maps do not provide the optimal parameters because no common minimum
209 spot was identified. Proper weighting for joint data treatment is difficult due to
210 differences in data quality. Nevertheless, comparison of the three rms distribution maps
211 may provide a clue for searching for reasonable parameters. For example, a source at a
212 depth of greater than 10 km with a deflation of 0.01 km^3 generates a smaller rms than a
213 shallower depth. No signal at TES station was also consistent with above assumption.
214 These considerations with respect to the rms maps suggest that the observed data might
215 be explained well by the possibility of a deeper source having a deflation volume of
216 approximately 0.01 km^3. A strain observation array with a proper station distribution is

217 required in order to clarify this problem numerically.

218 Takahashi and Miyamura (2009) found that the activity of DLEs in the Meakan-dake
219 volcano is the second highest among Japanese quaternary volcanoes. Source mechanism
220 studies of DLEs have suggested possible crack openings caused by fluid (Nakamichi et
221 al., 2003). Activation of DLEs prior to eruption or magmatic unrest had been reported at
222 several volcanoes (White, 1996, Nakamichi et al., 2003), and DLE activations without
223 successively eruption have also been reported (Nichols et al., 2011). In the
224 Meakan-dake volcano, more than 800 DLE events were recorded during the decade
225 before the 2008 earthquake swarm. The epicenters and DLEs were concentrated just
226 beneath the summit crater at depths of 20 km and 25 km, respectively (Takahashi and
227 Miyamura, 2009). These findings imply the possible presence of fluid and/or magma in
228 the DLE hypocenter region. The cumulative number of DLEs and shallow volcanic
229 earthquakes (SVEs) as determined by the JMA during the earthquake swarm is shown in
230 Fig. 8. An increase in the number of DLEs started the night of January 8 at a depth of
231 between 15 and 20 km nearly simultaneously with the water table decrease at the AK
232 wells.

233 The observed groundwater level and GPS data suggest a possible interaction between
234 deeper deflation and the shallow earthquake swarm. The rapid response of shallower
235 seismic activity to DLEs activations were observed during the Mt. Pinatubo (White,
236 1996) and Mt. Iwate (Nakamichi et al., 2003) unrests. In the Meakan-dake volcano, a
237 delay of only one day of shallower activity posteriori to the initiation of strain signals
238 implied that a possible upward volatile migration generated the swarm. However,
239 observed data that indicating no eruption, no change in smoke amount and active vent
240 temperature did not seem to support this idea (Fig. 2).

241 Self-potential surveys suggested a possible permeable layer at around sea level
242 (Matsushima et al., 1994, Zlotnicki and Nishida, 2003). Volcanic gases, e.g., H_2S, SO_4,
243 and CO_2, have high water solubility (National Astronomical Observatory of Japan,
244 2010). If we accept the hypothesis that upward volatile migration occurred as the water
245 table descended, then the lack of surface phenomena might suggest that the aquifer
246 acted as a barrier due to the dissolution of ascending volcanic volatiles in water.
247 Chemical component analysis of hot spring water 2 km west of the summit crater
248 reveals very higher concentration of H_2S to be 34.99 mg per liter and of SO_4 to be 1,615
249 mg per liter, respectively (Geological Survey of Hokkaido, 1980). This also implies
250 possible volcanic gas dissolution in the shallower aquifer. Continuous chemical
251 component analysis of hot spring water may provide clues to help clarify the interaction
252 between the shallower aquifer and volcanic volatile migration.
253 A schematic diagram of the possible volcano system of the Meakan-dake volcano is
254 shown in Fig. 9. The time series of the observation data, the existence and activation of
255 DLEs, the possible deflation of a deeper source, and the shallow seismic activity imply
256 a strong relationship between these phenomena. However, no obvious migration
257 processes, such as earthquakes, were documented along possible channels between the
258 deep and shallow active zones. This puzzling feature was also exhibited by the 1991 Mt.
259 Pinatubo catastrophic eruption (White, 1996). Unmodeled but likely mechanisms in
260 volcanic fields, e.g., viscoelastic and/or anelastic responses, should also be considered
261 in the future. Detailed monitoring by hydrologic and mechanical parameters is required
262 in order to confirm a realistic model that can fully explain observed data. A strain
263 observation array that has sensitivity to mid-crustal depth will be fundamental in order
264 to clarify the conduit process between the DLE epicenter and the shallower seismic

zone.

5. Conclusion

We have started groundwater level observations at intermittent hot spring wells near the active Meakan-dake volcano using a low-cost system. Simultaneous lowering of the water level prior to a volcanic earthquake swarm was recorded at three independent wells. The total volumetric strain changes associated with an earthquake swarm was 6 to 7×10^{-7}. Proper point source (Mogi model) parameters were sought using water level and GPS data. Although optimal parameters were not defined because of an insufficient data set, several assumption and residual distribution maps suggest a possible deflation source at a greater depth (>10 km) with a volume change of approximately 0.01 km^3. Synchronization in space and time between DLE activation and possible deflation source activity was recognized. Although the timeline of deeper activities and a shallower earthquake swarm might imply that the earthquake swarm was triggered by upward migrating volatile, no physical model or observation data were presented. The observation data of the present study clearly demonstrate low-cost groundwater level observation at existing wells can record volumetric strain with high precision, on the order of 10^{-7}. The proposed monitoring system can be easily expanded because of the numerous unused hot spring wells that exist near active volcanoes.

Acknowledgments

We are grateful to the anonymous reviewers for their helpful comments. We express our great thanks to the Maeda-Ippoen Foundation that allowed us to make observations at their hot spring wells at Akan-cho in Kushiro. We also express our gratitude to Mrs. T.

289 Suzuki and T. Takahashi at the Geological Survey of Hokkaido, and Mrs. M. Ichiyamagi,
290 M. Takada, and Prof. Kasahara of Hokkaido University, who helped us in carrying out
291 our observations. We are also thankful to Mrs. Miyamura and Oikawa and the staff of
292 the Sapporo District Meteorological Observatory of the Japan Meteorological Agency
293 who kindly allowed us to use hypocenter, earthquake, GPS, and temperature data. This
294 study was supported by the Ministry of Education, Culture, Sports, Science and
295 Technology (MEXT) of Japan under its Observation and Research Program for the
296 Prediction of Earthquakes and Volcanic Eruptions. GMT software (Wessel and Smith,
297 1995) was used for drawing pictures
298

299 **References**

300 Agnew, D., and F. Wyatt, 2003. Long-Base Laser Strainmeters: A Review, Scripps
301 Institution of Oceanography Technical Report, 54pp.

302 Akita, F., and N. Matsumoto, 2004. Hydrological responses induced by the Tokachi oki
303 earthquake in 2003 at hot spring wells in Hokkaido, Japan, Geophys. Res. Lett., 31,
304 L16603, doi:10.1029/2004GL020433.

305 Chardot, L., B. Voight, R. Foroozan, S. Sacks, A. Linde, R. Stewart, D. Hudayat, A.
306 Clarke, D. Elsworth, N. Fournier, J. C. Komorowski, G. Mattioli, R. S. J. Sparks,
307 and C. Widiwijayanti, 2010. Explosion dynamics from strainmeter and
308 microbarometer observation, Soufriere Hills Volcano, Moteserrat: 2008-2009,
309 Geophys. Res. Lett., 37, L00E24, doi10.1029/2010GL044661.

310 Gahalaut, K., V. K. Gahalaut, and R. K., Chadha, 2010. Analysis of coseismic
311 water-level changes in the wells in the Koyna-Warna region, western India, Bull.
312 Seism. Soc. Am., 100, 1389-1394.

313 Geological Survey of Hokkaido, 1980. Geothermal indications and hot springs of
314 Hokkaido, Japan (D) Eastern Area, 155pp.
315 Ishiguro, M., H. Akaike, M. Ooe, and S. Nakai, 1981. A Bayesian approach to the
316 analysis of earth tides, Proc. 9th Int. Sympos. Earth Tides, New York, pp.283-292,
317 ed. Kuo, J. T., Schweizerbart'sche Verlangsbuchhandlung, Stuttgart.
318 Itaba, S., N. Koizumi, N. Matsumoto and R. Ohtani, 2010. Continuous observation of
319 groundwaters and crustal deformation for forecasting Tonankai and Nankai
320 earthquakes in Japan, Pure Appl. Geophys., 167, 1105-1114.
321 Kawamori, H., K. Fujimoto, T. Takahashi, and H. Wakayama, 1987. The report on
322 geothermal well drilling in Akan Lake-side, Hokkaido (AK1), 59, 119-131.
323 Matsumoto, K, T. Sato, T. Takanezawa and M. Ooe, 2001. GOTIC2: A program for
324 computation of oceanic tidal loading effect, J. Geod. Soc. Japan, 47, 243-248.
325 Matsumoto, N., 2002. Regression analysis for anomalous changes of ground water level
326 due to earthquake, Geophys. Res. Lett., 19, 1193-1196.
327 Matsumoto, N., G. Kitagawa and E. Roeloffs, 2003. Hydrological response to
328 earthquakes in the Haibara well, central Japan–I. Groundwater level changes
329 revealed using state space decomposition of atmospheric pressure, rainfall and tidal
330 responses, Geophys. J. Int., 155, 885-898.
331 Matsushima, N., N. Okazaki, R. Ichikawa, M. Michiwaki and Y. Nishida, 1994.
332 Electromagnetic and geothermal surveys on Me-akan volcano, Geophys. Bull.
333 Hokkaido Univ., 57, 1-10.
334 Mogi, K., 1958. Relation between the Eruption of Various Volcanoes and the
335 Deformation of the Ground Surface around them, Bull. Earthq. Res. Ins., 36,
336 99-134.

337 Nakamichi H., H. Hamaguchi, H. Tanaka, S. Ueki, T. Nishimura and A. Hasegawa,
338 2003. Source mechanism of deep and intermediate-depth low-frequency
339 earthquakes beneath Iwate volcano, northern Japan, Geophys. J. Int., 154, 811-828.
340 National Astronomical Observatory of Japan ed., 2009. Chronological Scientific Table
341 2010, Maruzen cooperation, 1041pp.
342 Nichols, M. L., S. D. Malone, S. C. Moran, W. A. Thelen, and J. E. Vidale, 2011. Deep
343 long-period earthquakes beneath Washington and Oregon volcanoes, J. Volcano.
344 Geotherm. Res., 200, 116-128.
345 Okada, Y., 1992. Internal deformation due to shear and tensile faults in a half space,
346 Bull. Seism. Soc. Am., 82, 1018-1040.Quilty E., and E. A. Roeloffs, 1997. Water
347 level changes in response to the December 20, 1994 M4.7 earthquake near
348 Parkfield, California, Bull. Seism. Soc. Am., 87, 310-317.
349 Quilty E., and E. A. Roeloffs, 1997. Water level changes in response to the December
350 20, 1994 M4.7 earthquake near Parkfield, California, Bull. Seism. Soc. Am., 87,
351 310-317.
352 Roeloffs, E., 1988. Hydrologic precursors to earthquakes: A review, Pure Appl.
353 Geophys., 126, 177-209.
354 Saito, T., 2008. Responses of the groundwater level to crustal strain: observation of 1Hz
355 sampling at Akan hot-spring wells in Hokkaido, Japan, Master thesis of Hokkaido
356 University, 72pp.
357 Shibata, T., N. Matsumoto, F. Akita, N. Okazaki, H. Takahashi and R. Ikeda, 2010.
358 Linear poroelasticity of groundwater levels from observational records at wells in
359 Hokkaido, Japan, Tectonophys., 483, 305-309.
360 Takahashi, H. and J. Miyamura, 2009. Deep low-frequency earthquakes occurring in

Japanese Islands, Geophys. Bull. Hokkaido Univ., 72, 177-190.

Tamura, Y, T. Sato, M. Ooe, and M. Ishiguro, 1991. A procedure for tidal analysis with a Bayesian information criterion, Geophys. J. Int., 104, 507-516.

Ueda, H., E. Fujita, M. Ukawa, E. Yamamoto, M. Irwan, and F. Kimata, 2005. Magma intrusion and discharge process at the initial stage of the 2000 activity of Miyakejima, Central Japan, inferred from tilt and GPS data, Geophys. J. Int., 161, 891-906, doi: 10.1111/j.1365-246X.2005.02602.x.

Wada,K., 1991. Mixing and evolution of magmas at Me-Akan volcano, eastern Hokkaido, Japan, Jour. Volcano. Soc. Japan, 36, 61-78.

Wada, K., C. Inaba and Y. Nemoto, 1997. Eruption history of Me-akan volcano, eastern Hokkaido, during the last 12000 years, Abstract of Volcanological Society of Japan meeting, P16.

Wakita, H., 1975. Water wells as possible indicators of tectonic strain, Science 189, 553–555.

White, R. A., 1996. Precursory deep long-period earthquakes at Mount Pinatubo. In: Newhall, C. G., Punongbayan, R. S. (Eds.), Fire and Mud: Eruptions and Lahars of Mount Pinatubo, Philippines, Univ. of Washington Pres, Seattle, pp207-326.

Yamaguchi, T., M. Kasahara, H. Takahashi, M. Okayama, M. Takada, and M. Ichiyanagi, 2010. Development of crustal deformation database system, Jour. Geodetic. Soc. Japan, 56, 47-58.

Zlotnicki, J., and Y. Nishida, 2003. Review on morphological insights of self-potential anomalies on volcanoes, Surv. Geophys., 24, 291-338.

Wessel, P., and W. H. F. Smith, New version of the generic mapping tools released, EOS Trans. AGU, 76(33), 329-336, 1995.

385

386 **Figure captions**

387 Fig. 1 (a) Map showing the geographical location of the Meakan-dake volcano
388 indicating the tectonic background. The dashed lines show the plate boundaries. (b)
389 Close-up of the rectangular area shown in Fig. 1(a). The nearest TES strain station
390 and GPS station (0496) are also indicated. (c) Location of well stations (AK1, AK3,
391 and AK4), GPS stations (0497, 9014, 0561, and 0182), and active vent 96-1, at
392 which temperature observations were made. An inset rectangular is used in Fig. 2.

393 Fig. 2 (a) Number of volcano earthquakes per day, and (b) temperature recorded at
394 active vent 96-1 crater shown in Fig. 1(c), from January 2000 to October 2008.

395 Fig. 3 Hypocenter distribution of the earthquake swarm from January 9 to 11, 2008, as
396 determined by the Sapporo District Meteorological Observatory of the Japan
397 Meteorological Agency. Hypocenters were estimated using data from more than
398 four stations. The horizontal and origin time errors were less than 400 m and 0.2 s,
399 respectively.

400 Fig. 4 Baseline length changes between the GPS stations shown in Fig. 1.

401 Fig. 5 Time series of the original water level, barometric pressure, and corrected water
402 level by BAYTAP-G at the AK1 station for two weeks before and after the
403 earthquake swarm of January 9 through 11, 2008.

404 Fig. 6 Water level data of the AK1, AK3 and AK4 wells. Tidal effects were eliminated
405 using BAYTAP-G tidal analysis software. Dilatational strain records at the TES
406 station, and the number of earthquakes per hour as counted by the Sapporo District
407 Meteorological Observatory of the Japan Meteorological Agency are also indicated.
408 The initiation of the water table fall of AK1 and the initiation of the earthquake

swarm are indicated by dotted and dashed lines, respectively.

Fig. 7 The rms residual distribution maps. (a) the rms summation of each GPS baseline, (b) the rms summation of each GPS vertical component, and (c) the rms of volumetric strain change of AK1. Contouring is performed using a normalized apparent rms value for each data type.

Fig. 8 Cumulative number of deep, low-frequency earthquakes (DLE), and shallow volcanic earthquakes (SVE).

Fig. 9 Schematic diagram of the volcanic unrest during January 2008. DLE: deep, low-frequency earthquake, SVE: shallow volcanic earthquake. Note that no earthquakes were observed between the deep and shallow active zones during the swarm period.

Table

Click here to download Table: Table.pdf

Table 1 Parameters of observation wells.

ID	Location (Lat, Lon, Height)	Depth (m)	Strainer depth (m)	Geology along strainer	Volumetric strain coefficient ($mm/10^{-8}$strain)	Water level change (cm)	Volumetric strain change (microstrain)
AK1	N43.4309 E144.0995 H432m	1061	518.1-1005.8: Casing	Miocene volcanic rocks	3.42	-19.2	-0.56
AK3	N43.4306 E144.0847 H420m	91.8	24.0-68.0: Casing Below 68.0: Bare	Pliocenne-Quaternary volcanic rocks	(0.38-0.50)	-2.8	-
AK4	N43.4303 E144.0846 H420m	54.7	41-54.7: Casing	Pliocenne-Quaternary volcanic rocks	0.60	-4.4	-0.74

Coefficient of AK3 is deduced from swarm-related water change comparing to AK1 and AK4.

Figure

Click here to download Figure: Fig, 1.pdf

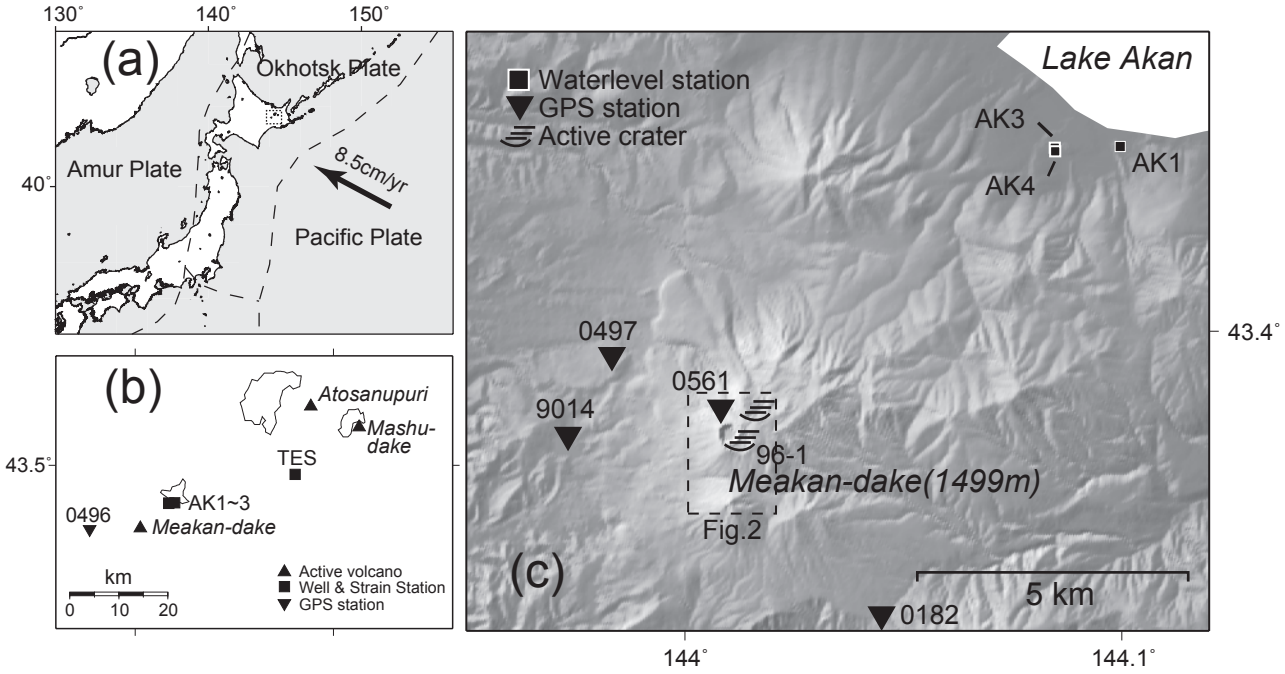

Fig. 1

Figure
Click here to download Figure: Fig. 2.pdf

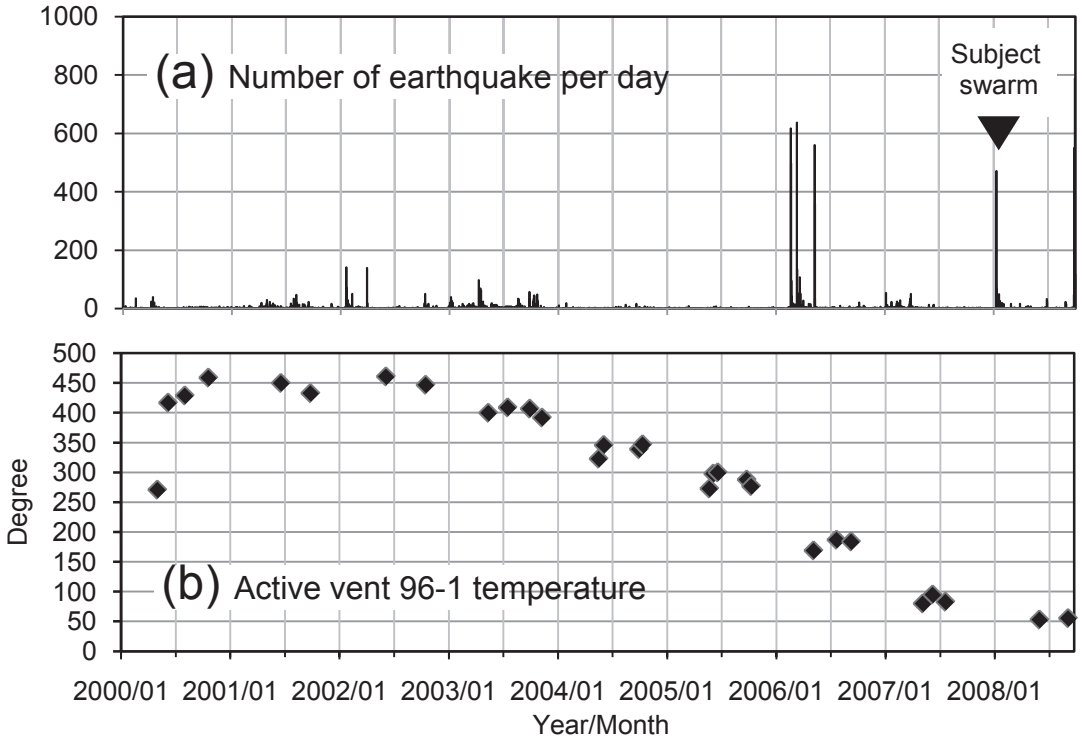

Fig. 2

Figure
Click here to download Figure: Fig. 3.pdf

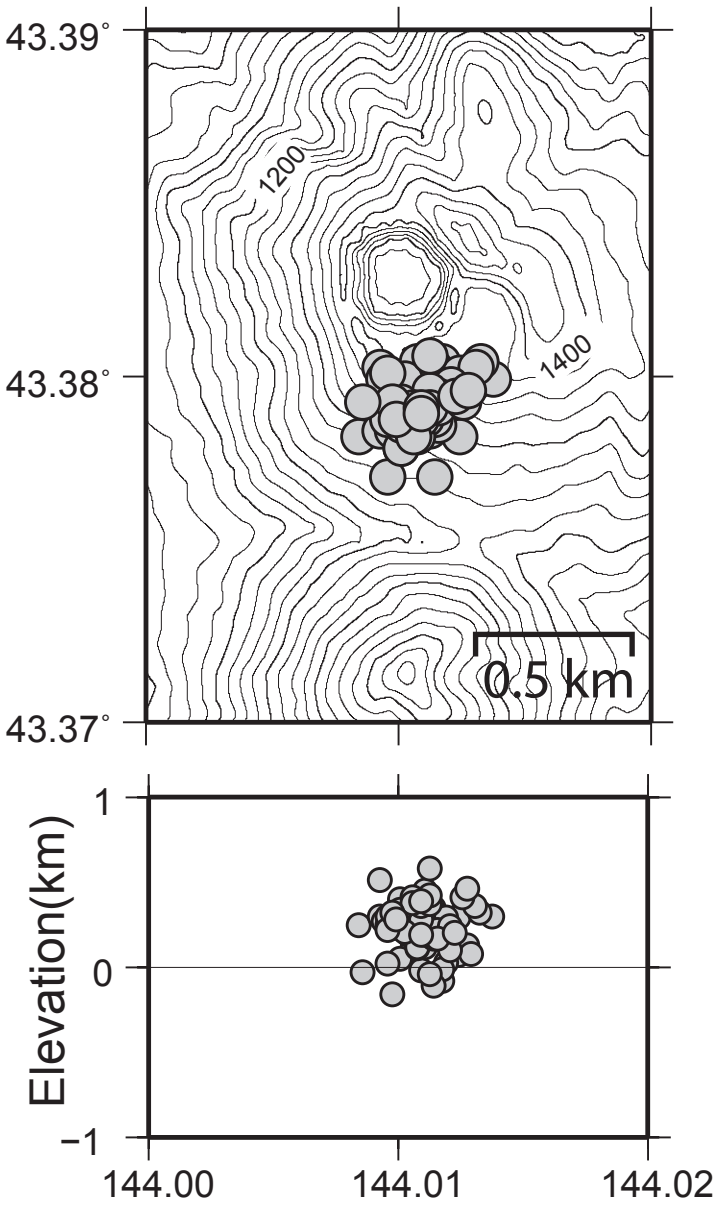

Fig. 3

Figure

Click here to download Figure: Fig. 4.pdf

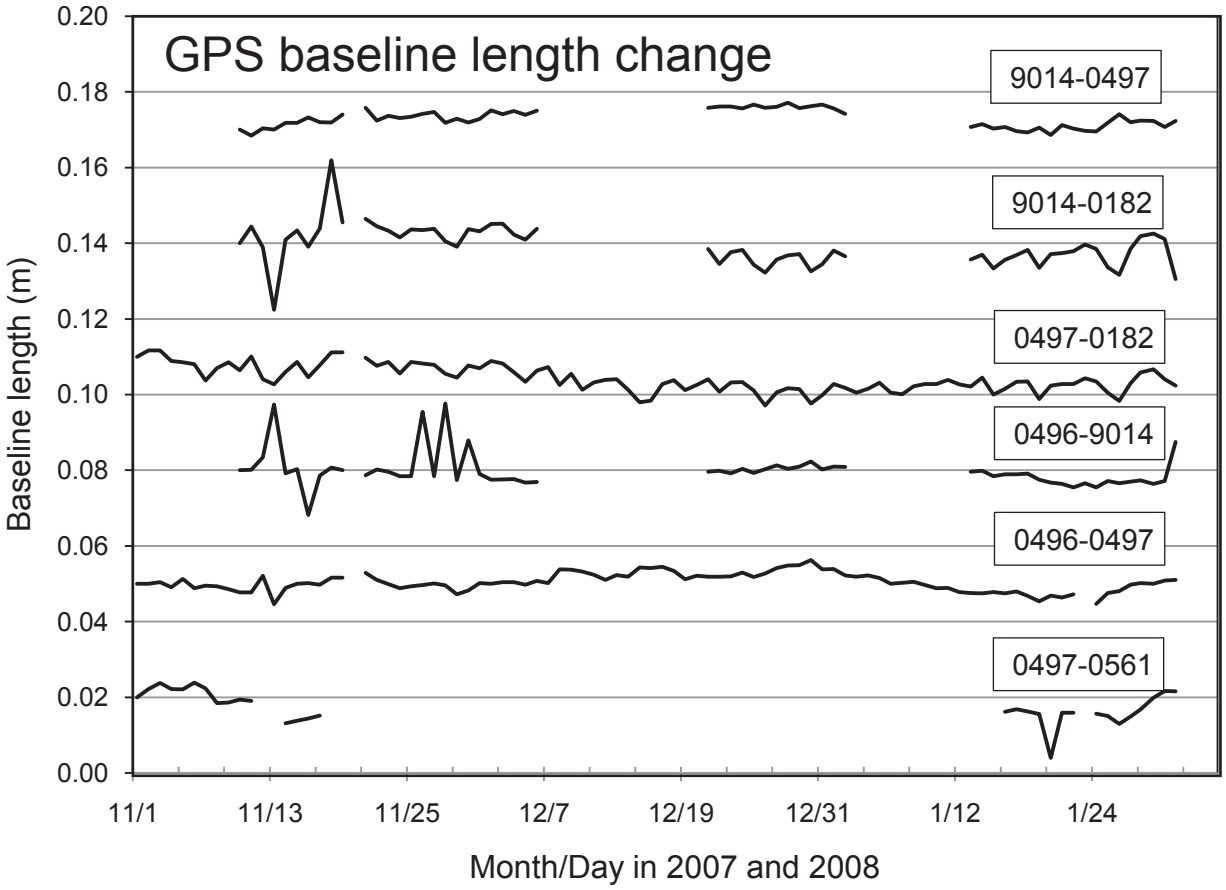

Fig. 4

Figure

Click here to download Figure: Fig. 5.pdf

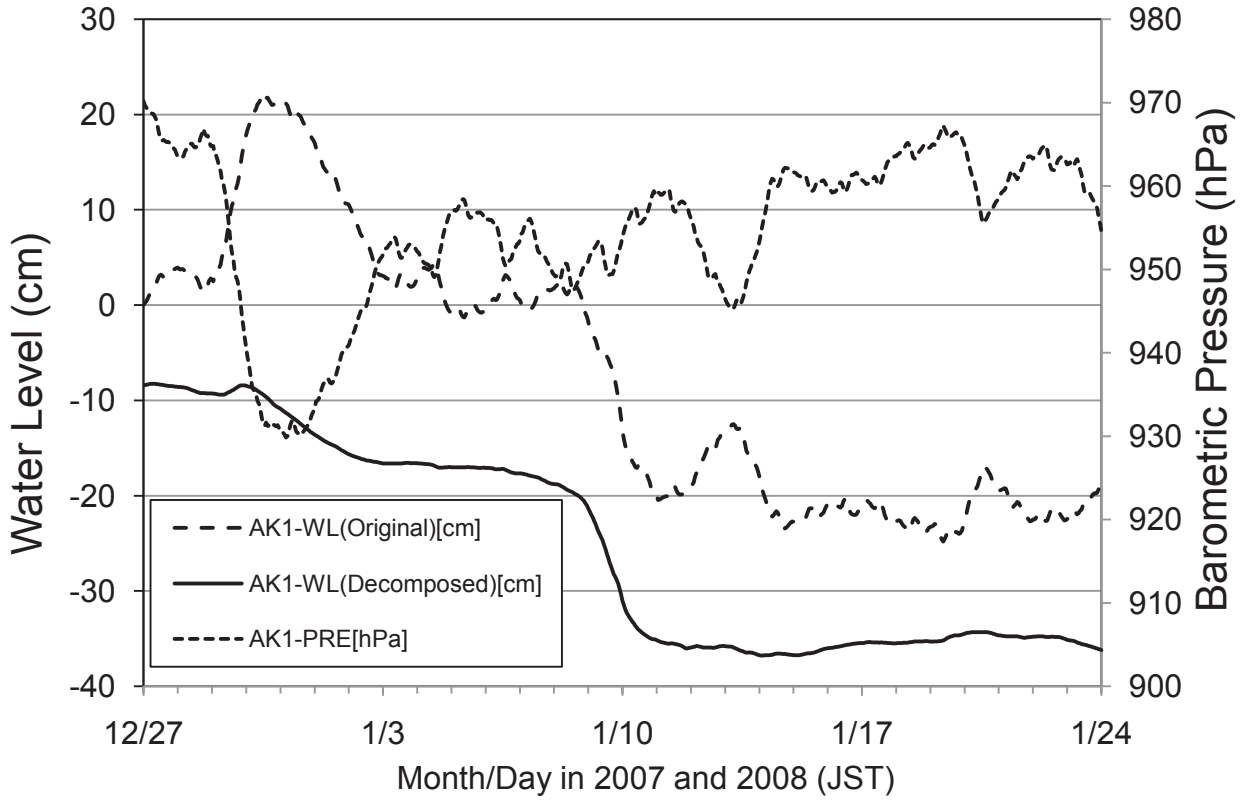

Fig. 5

Figure
Click here to download Figure: Fig. 6.pdf

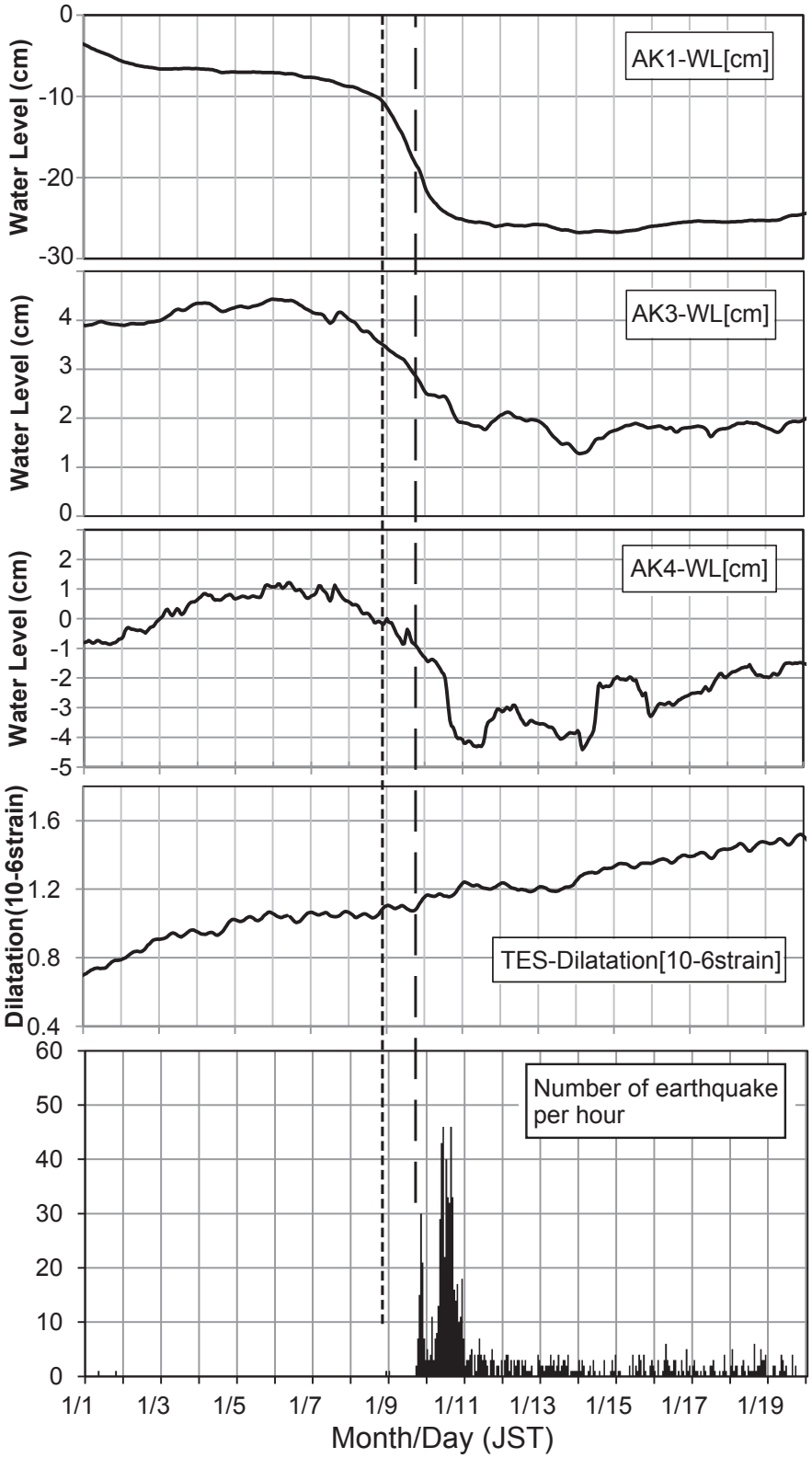

Fig. 6

Figure

Click here to download Figure: Fig. 7.pdf

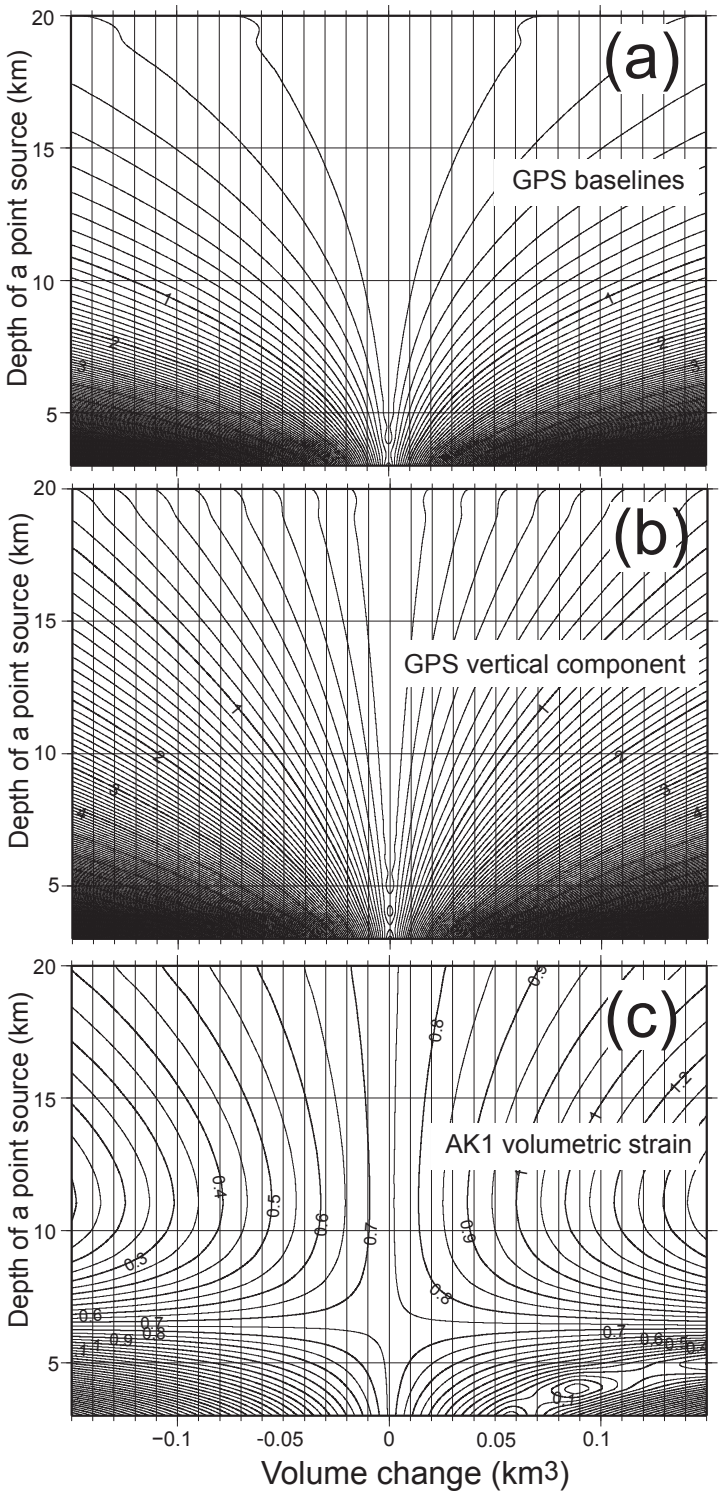

Fig. 7

Figure

Click here to download Figure: Fig. 8.pdf

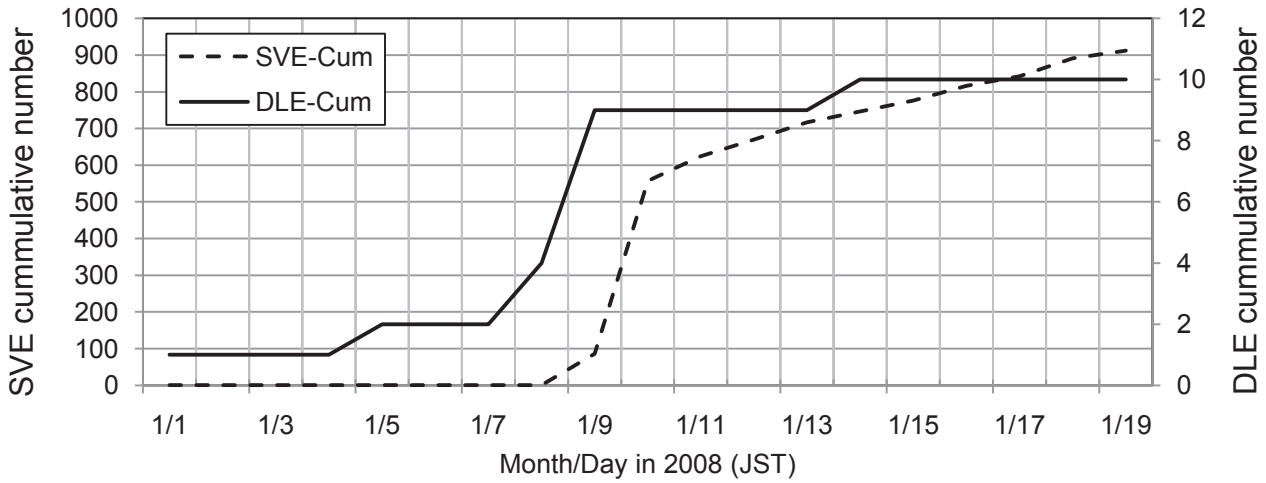

Fig. 8

Figure
Click here to download Figure: Fig. 9.pdf

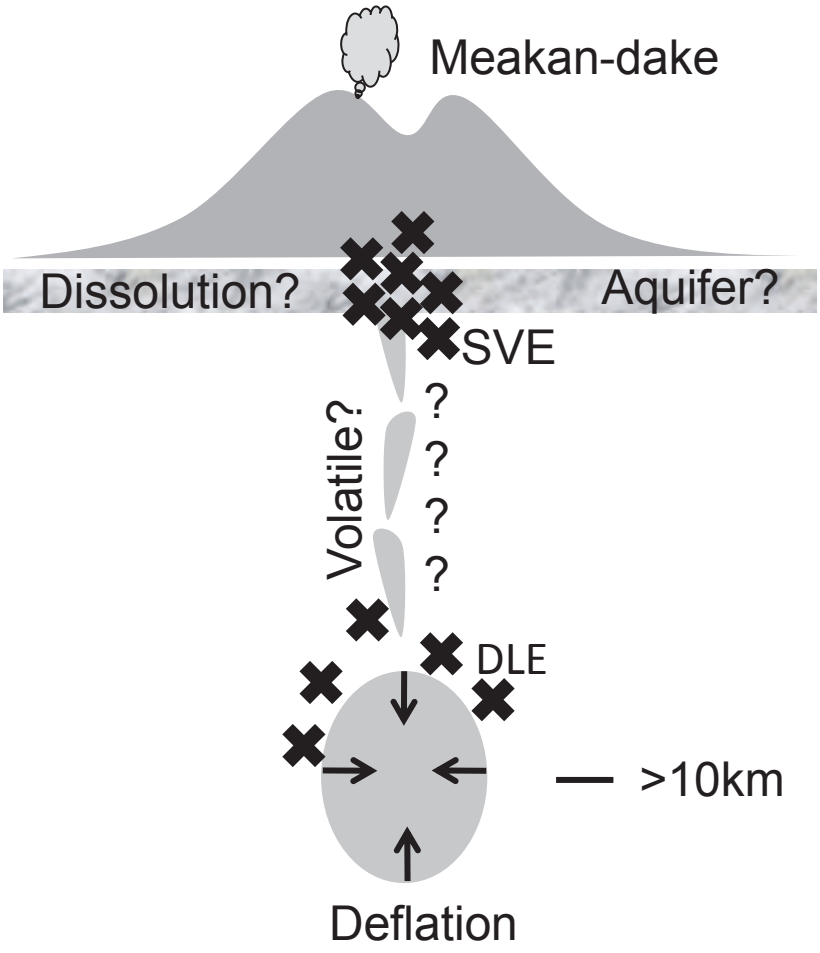

Fig. 9